Available online at www.sciencedirect.com
SCIENCE DIRECT®
International Journal of Heat and Mass Transfer 48 (2005) 3140–3150
International Journal of HEAT and MASS TRANSFER
www.elsevier.com/locate/ijhmt

A semi-empirical model for estimating permeability and inertial coefficient of pin-fin heat sinks

Tzer-Ming Jeng [a], Sheng-Chung Tzeng [b,*]

[a] Department of Mechanical Engineering, Air Force Institute of Technology, GangShan 820, Taiwan, ROC
[b] Department of Mechanical Engineering, Chienkuo Technology University, No. 1, Chien Shou N Road, Changhua 500, Taiwan, ROC

Received 15 October 2004; received in revised form 4 February 2005
Available online 18 April 2005

Abstract

This work presents a novel semi-empirical model for estimating the permeability and inertial coefficient of pin-fin heat sinks that are set as porous media. The forms of correlations for the permeability and inertial coefficient of pin-fin heat sinks are firstly derived theoretically, then a series of pressure drop tests are performed for modifying those correlations. The variable parameters of pin-fins studied herein are the relative longitudinal pitch, the relative transverse pitch, the relative fin height and the relative fin length. The present correlations are reasonable by comparing with the data of other tests. Additionally, within the range of Reynolds number (Re_d = 676–11,252), at a given Re_d, the effect of the relative fin height on the pressure drop is negligible. The pressure drop declines as the relative fin length increases, especially as the relative transverse pitch and the relative longitudinal pitch increase. It increases as the relative transverse pitch declines or the relative longitudinal pitch increases.

Keywords: Permeability; Inertial coefficient; Pin-fin heat sink; Porous medium; Pressure drop

1. Introduction

The trend in the electronic equipment industry toward denser and more powerful products depends on better cooling technology. An assembly of pin-fin heat sinks and fans is the most popular cooling device because its configuration is simple and it is cheap. The conventionally numerical model to simulate the flow and thermal behavior of pin-fin heat sinks in rectangular channels is to employ the Navier–Stokes equation and the energy equation. Much computer time is required because a three-dimensional calculation is involved. Finned heat sinks contain many regularly arranged fins, which can be regarded as constituting a porous structure. Accordingly, this "porous approach" can be applied to simplify a numerical study.

Koh and Colony [1] modeled the microstructure as a porous medium, using Darcy's law to describe the flow. Vafai and Tien [2] employed the modified Darcy equation to explain the boundary effect in convection problems. Koh and Colony [3] extended the analytical porous approach to microchannels. You and Chang [4] combined experimental data to numerically determine the heat transfer coefficient for a square pin-fin channel

* Corresponding author. Tel.: +886 4 7111 111x3132; fax: +886 4 7357 193.
E-mail addresses: tsc@ctu.edu.tw, tsc33@ms32.hinet.net (S.-C. Tzeng).

0017-9310/$ - see front matter © 2005 Elsevier Ltd. All rights reserved.
doi:10.1016/j.ijheatmasstransfer.2005.02.016

Nomenclature

C	friction coefficient of passages between fins
C'	friction coefficient of the channel
Da	Darcy number, $Da = K/d^2$
D_h	hydraulic diameter of passages between fins, $D_h = 4Hs/2/(H + s)$, [m]
D'_h	hydraulic diameter of the channel, $D'_h = 4HW/2/(H + W)$, [m]
d	fin thickness or diameter of circular pin-fin, [m]
d^*	length of the pin-fin along the streamwise direction, [m]
F	inertial coefficient
f_d	friction factor, $f_d = \frac{\Delta P}{0.5\rho u^2}\frac{d}{L}$
H	height of the heat sink, [m]
K	permeability, [m^2]
Kc	contraction loss coefficient
Ke	expansion loss coefficient
L	length of the heat sink, [m]
n	the number of fin rows in the flow direction
Re_d	Reynolds number, $Re_d = \rho u d/\mu$
Re_D	Reynolds number, $Re_D = \rho u D_h/\mu/(1 - X_T^{-1})$
Re'_D	Reynolds number, $Re'_D = \rho u D'_h/\mu$
s	transverse inter-fin spacing, [m]
s^*	longitudinal inter-fin spacing, [m]
S_L	center-to-center longitudinal distance between the adjacent fins, [m]
S_T	center-to-center transverse distance between the adjacent fins, [m]
u	average Darcy velocity, [m/s]
u^*	actual average aperture velocity, [m/s]
W	width of the heat sink, [m]
X_L	relative longitudinal pitch, S_L/d^*
X_T	relative transverse pitch, S_T/d
ΔP	pressure drop, [Pa]

Greek symbols

χ	ratio of the channel skin friction to the fin skin friction
ε	porosity
ϕ	the factor to correct the pressure losses at the entrance and exit of internal fin rows
μ	viscosity, [kg/m/s]
ρ	density, [kg/m^3]

Subscripts

EF	extruded-fin
PF	pin-fin

flow, by applying the non-Darcian model, which incorporates the effect of the inertial coefficient. Kim and Kim [5] provided analytical solutions for both velocity and temperature profiles in micro channel heat sinks using the modified Darcy model of the micro channel heat sink as a fluid-saturated porous medium. Recently, Kim and Kim [6] and Kim et al. [7] modeled the straight fin heat sink and the pin-fin heat sink as a porous medium, respectively.

The characteristics of porosity, such as the permeability and the inertial coefficient, need to be determined, before fluid flow and heat transfer can be numerically analyzed using the Darcy or non-Darcian model. Bear [8] and Bear and Verruijt [9] presented the detail derivation of the Darcy law and its extensions. Besides, Ergun [10] provided the famous correlations for the permeability and the inertial coefficient. However, they found correlations for packed spherical beds, not for parallel fin structures. Drummond and Tahir [11], Fowler [12] and Martin et al. [13], found some correlations for the permeability of square arrays of parallel cylinders. The aforementioned correlations have been applied in numerical studies of porous media. However, without a correlation for the inertial coefficient, it cannot be applied to Forchheimer or nonlinear flow. Zukauskas and Ulinskas [14] experimentally investigated the pressure drop and heat transfer by forced convection in tube banks for various distances between tubes. You and Chang [15] experimentally obtained the porous flow characteristics for air flow through uniformly distributed square pin-fins. They did not provide systematic results for the permeability or inertial coefficient of fin arrays. In the work of Kim and Kim [6], the permeability of the straight fin heat sink was determined analytically from forced convective flow between infinite parallel plates. The permeability and the inertial coefficient of the pin-fin heat sink, reported by Kim et al. [7], were decided experimentally and correlations for them were provided. Although Kim and Kim [6] and Kim et al. [7] almost completed the work to model the finned heat sink as a porous medium, they did not extend the analysis of the straight fin heat sink to analyze the pin-fin heat sink. Hence, the correlations for the permeability and the inertial coefficient of the pin-fin heat sink were polynomials. Additionally, Kim et al. [7] employed the method presented by You and Chang [15] to determinate the permeability and the inertial coefficient. The method of You and Chang [15] decided the permeability and the inertial coefficient by matching the numerical results with the experimental data. It was more complex than the method reported by Hunt and Tien [16]. Moreover, both methods of You and Chang [15] and Hunt and Tien [16] needed experiments conducted over a wide range of flow rates, including the very small flow rates to

identify the permeability of the pin-fin heat sink with a large porosity. In fact, the measurement of pressure drop at a very small flow rate is difficult and uncertainty. Then the results obtained from above two methods may be only applied to Forchheimer flow.

This work provides analytical expressions for the permeability and inertial coefficient of pin-fin heat sinks. Additionally, the pressure drops across the pin-fin heat sinks in rectangular channels are experimentally explored. The variable parameters are the relative longitudinal pitch (X_L), the relative transverse pitch (X_T), the relative fin height (H/d) and the relative fin length (d^*/d). Then, a semi-empirical model for estimating the permeability and inertial coefficient of pin-fin heat sinks is provided using the analytical expressions and the experimental data. Since the permeability in the present model is derived analytically, a measurement of pressure drop at a very small flow rate is unnecessary. The results are compared to those of other tests to verify the accuracy of the prediction using the semi-empirical equations for the permeability and inertial coefficient proposed herein. Therefore, the compact finned heat sinks can be regarded as the porous media and analyzed using the porous approach.

2. Similarity between pin-fin heat sinks and porous media

This work concerns the extruded-fin heat sink and the pin-fin heat sink with the in-line array. Fig. 1 presents the configuration of the presented pin-fin heat sinks.

2.1. Extruded-fin heat sinks

The total pressure drop across an extruded-fin heat sink is the sum of the pressure drop at the entrance ($=1/2\rho u^{*2}[1-\sigma_{EF}+Kc_{EF}]$), the pressure drop across the region between the fins ($=1/2\rho u^{*2}\{[C/Re_D]\cdot[L/D_h]\}$) and the pressure recovery at the exit ($=-1/2\rho u^{*2}[1-\sigma_{EF}-Ke_{EF}]$). It can be expressed as follows:

$$\Delta P_{EF}=\frac{1}{2}\rho u^{*2}\left[(Kc_{EF}+Ke_{EF})+\frac{C}{Re_D}\frac{L}{D_h}\right] \tag{1}$$

where u^* is the actual average aperture velocity in the region between the fins; Kc_{EF} is the convergence coefficient at the inlet; Ke_{EF} is the divergence coefficient at the exit; C is the friction coefficient (i.e. $f_D Re_D = C$); L the length of the heat sink; D_h is the hydraulic diameter of the passage between the fins, and $Re_D = \rho u^* D_h/\mu$.

If the extruded-fin heat sink is regarded as a porous medium, then Eq. (1) can be rearranged to determine an equation for the average pressure drop over length of the heat sinks, like that of the Darcy–Forchheimer Model, which governs flow through porous media. It is rewritten as follows and the detail can be found in Appendix A.

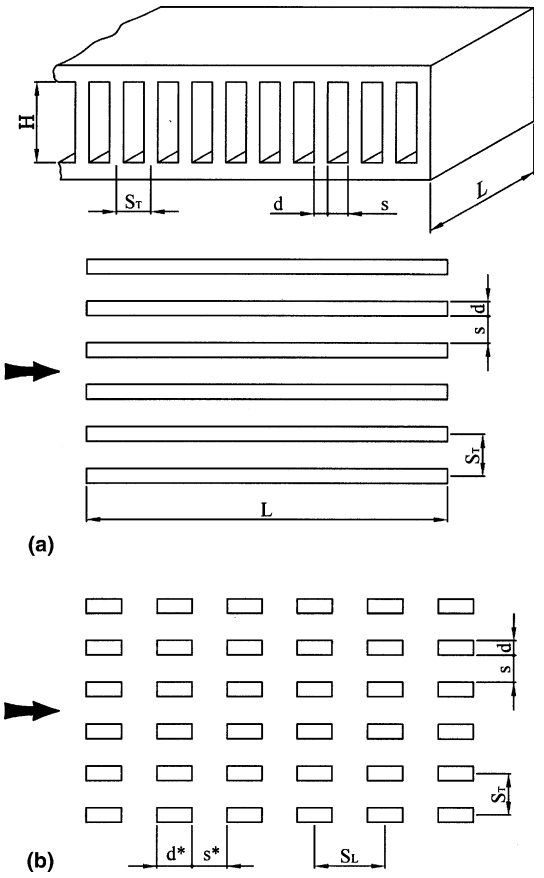

Fig. 1. Configuration of the present pin-fin heat sinks. (a) Extruded-fin heat sink (top view) and (b) pin-fin heat sink (top view).

$$\frac{\Delta P_{EF}}{L}=\frac{\mu}{K_{EF}}u+\frac{\rho F_{EF}}{\sqrt{K_{EF}}}u^2 \tag{2}$$

$$K_{EF}=\frac{2D_h^2(1-X_T^{-1})}{C} \tag{3}$$

$$F_{EF}=\frac{D_h}{L}\sqrt{\frac{1}{2C}}\frac{1}{(1-X_T^{-1})^{1.5}}(Kc_{EF}+Ke_{EF}) \tag{4}$$

where K_{EF} is the permeability and F_{EF} is the inertial coefficient for the extruded-fin heat sink; u represents the average inlet velocity ($=u^*(1-X_T^{-1})$), and X_T is the relative transverse pitch ($X_T = S_T/d$, S_T is the center-to-center transverse distance between the adjacent fins and d is the thickness of each fin).

For laminar flow, the friction coefficient C can be determined from the curve fitted to the results of Mills [17] for rectangular channels. Besides, the friction coefficient C for turbulent flow can be determined from an

empirical formula presented by Chapman [18]. These correlations are as follows:

$$C_{la} = 31.72 \cdot \zeta^2 - 55.85 \cdot \zeta + 80.94 \quad \text{for laminar flow} \quad (Re_D \leqslant 2000) \tag{5A}$$

$$C_{tu} = 0.3164 \cdot Re_D^{0.75} \quad \text{for turbulent flow} \quad (Re_D \geqslant 10000) \tag{5B}$$

where ζ is the ratio of D_h to s (where D_h is the hydraulic diameter of the passage between the fins and s is the inter-fin spacing). Therefore, C can be estimated for transition flow using the interpolation method.

An equation experimentally derived by Mills [17] is used to predict Kc_{EF} and Ke_{EF}.

$$Kc_{EF} = 0.4 \cdot (1 - \sigma_{EF}^2) + \beta_{EF} \tag{6}$$

$$Ke_{EF} = (1 - \sigma_{EF})^2 - \beta_{EF} \cdot \sigma_{EF} \tag{7}$$

In Eqs. (6) and (7), $\sigma_{EF}(= 1 - X_T^{-1})$ represents the porosity of the extruded-fin heat sink. The value of β_{EF} is a function of the geometry of the passage. The data for parallel plates and square passages yield the relationship between β_{EF} and C using the interpolation method.

$$\begin{aligned}\beta_{EF} &= -0.01 \cdot (C - 57) + 0.79 \quad \text{for } Re_D < 2 \times 10^3 \\ &= -0.002 \cdot (C - 57) + 0.18 \quad \text{for } 2 \times 10^3 \leqslant Re_D < 6 \times 10^3 \\ &= -0.0015 \cdot (C - 57) + 0.12 \quad \text{for } 6 \times 10^3 \leqslant Re_D < 6 \times 10^4 \\ &= 0 \quad \text{for } Re_D \geqslant 6 \times 10^4\end{aligned} \tag{8}$$

It needs to note that the C in Eq. (8) employs the correlation of Eq. (5A) for all range of Re_D. For an extruded-fin heat sink, the porosity ε just equals $(1 - X_T^{-1})$. If the height of each fin is assumed to exceed greatly the inter-fin spacing (so $H \gg s$), the hydraulic diameter is expressed as follows:

$$D_h = \frac{2\varepsilon}{1 - \varepsilon} d \tag{9}$$

Substituting Eq. (9) into Eqs. (3) and (4) yields equations for the permeability and inertial coefficient of the extruded-fin heat sink with $H \gg s$.

$$K_{EF} = \frac{8\varepsilon^3 d^2}{C(1 - \varepsilon)^2} \tag{10}$$

$$F_{EF} = \frac{1}{\sqrt{C/2}} \frac{d}{L} \frac{1}{(1 - \varepsilon)\sqrt{\varepsilon}} (Kc_{EF} + Ke_{EF}) \tag{11}$$

2.2. Pin-fin heat sinks

A pin-fin heat sink may be assumed to contain n rows of extruded-fin heat sinks. The total pressure drop across a pin-fin heat sink is the summation of those across the arrays of extruded-fin heat sinks. Because the pressure changes at the inlet and exit of the pin-fin heat sinks are different from those of internal fin rows, the former would be treated separately from the latter. The detail can be found in Appendix A. Hence, the pressure drop across a pin-fin heat sink, determined from Eqs. (2)–(4), is,

$$\frac{\Delta P_{PF}}{L} = \frac{\mu}{K_{PF}} u + \frac{\rho F_{PF}}{\sqrt{K_{PF}}} u^2 \tag{12}$$

$$K_{PF} = \frac{2D_h^2 (1 - X_T^{-1})}{(1 + \chi) C (X_L^{-1})} \tag{13}$$

$$F_{PF} = \frac{D_h}{d^*} \sqrt{\frac{1}{2(1 + \chi)C}} \frac{(X_L^{-1})^{0.5}}{(1 - X_T^{-1})^{1.5}} \frac{1 + (n - 1)\phi}{n} \times (Kc_{EF} + Ke_{EF}) \tag{14}$$

where ΔP_{PF} is the total pressure drop across the pin-fin heat sink; L is the length of the pin-fin heat sink, and X_L

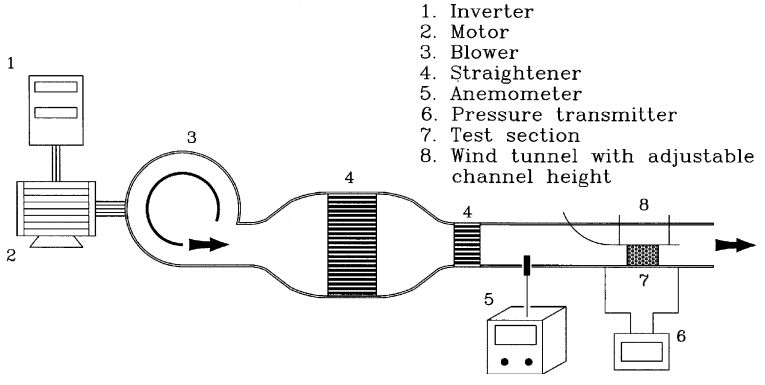

Fig. 2. Experimental setup.

is the relative longitudinal pitch. ($X_L = S_L/d^*$ where S_L is the center-to-center longitudinal distance between the adjacent fins and d^* is the length of the pin-fin in the direction of the stream.) The term C is the friction coefficient and evaluated by using Eq. (5). The term χ is the ratio of the channel skin friction to the fin skin friction and evaluated by using Eq. (A.3). The term n is the number of fin rows in the flow direction. The term $\phi(\leqslant 1)$ is an empirical factor that corrects the pressure losses (or the form drag) at the entrance and exit of internal fin rows. It may be a function of X_T and s^*. The value of ϕ will be discussed in Section 4.

If $d = d^*$ is assumed, and the height of fin is assumed to be much larger than the inter-fin spacing ($H \gg s$), then the hydraulic diameter is expressed as follows:

Table 1
List of input parameters and semi-empirical results

Case no.	Input parameters					Semi-empirical results			
	H/d	X_T	X_L	d^*/d	n	ϕ	χ	K [m^2]	F
a1	10	1.5	1.5	1	20	0.222	0.0007	6.47E−07	6.79E−02
a2	10	1.5	2	2	8	0.962	0.0014	8.62E−07	1.12E−01
a3	10	1.5	3	5	2	0.904	0.0028	1.29E−06	3.59E−02
a4	10	2	1.5	2	10	0.184	0.0041	3.75E−06	2.55E−02
a5	10	2	2	5	3	0.877	0.0081	4.98E−06	3.06E−02
a6	10	2	3	1	10	0.501	0.0162	7.41E−06	7.47E−02
a7	10	3	1.5	5	4	0.563	0.0202	1.84E−05	1.97E−02
a8	10	3	2	1	15	0.176	0.0404	2.40E−05	2.91E−02
a9	10	3	3	2	5	0.794	0.0807	3.46E−05	4.21E−02
a10	10	1.5	1.5	2	10	0.521	0.0007	6.47E−07	7.62E−02
a11	10	1.5	3	2	5	1.074	0.0028	1.29E−06	1.00E−01
a12	10	2	1.5	5	4	0.539	0.0041	3.75E−06	2.52E−02
a13	10	2	3	5	2	0.890	0.0162	7.41E−06	2.54E−02
a14	10	3	1.5	1	20	0.043	0.0202	1.84E−05	1.35E−02
a15	10	3	3	1	10	0.587	0.0807	3.46E−05	6.35E−02
b1	5	1.5	1.5	1	20	0.209	0.002	6.27E−07	6.42E−02
b2	5	1.5	2	2	8	0.944	0.004	8.34E−07	1.06E−01
b3	5	1.5	3	5	2	1.040	0.008	1.25E−06	3.68E−02
b4	5	2	1.5	2	10	0.207	0.0111	3.47E−06	2.65E−02
b5	5	2	2	5	3	0.793	0.0223	4.58E−06	2.75E−02
b6	5	2	3	1	10	0.517	0.0446	6.72E−06	7.30E−02
b7	5	3	1.5	5	4	0.664	0.0503	1.51E−05	2.01E−02
b8	5	3	2	1	15	0.206	0.1006	1.92E−05	2.95E−02
b9	5	3	3	2	5	0.814	0.201	2.64E−05	3.78E−02
b10	5	1.5	1.5	5	4	0.993	0.002	6.27E−07	5.10E−02
b11	5	1.5	2	5	3	1.071	0.004	8.34E−07	4.65E−02
b12	5	2	1.5	1	20	0.047	0.0111	3.47E−06	1.78E−02
b13	5	2	2	1	15	0.178	0.0223	4.58E−06	3.73E−02
b14	5	3	1.5	2	10	0.176	0.0503	1.51E−05	1.74E−02
b15	5	3	2	2	8	0.450	0.1006	1.92E−05	2.96E−02
c1	2	1.5	1.5	1	20	0.203	0.0096	5.57E−07	5.96E−02
c2	2	1.5	2	2	8	0.839	0.019	7.36E−07	9.54E−02
c3	2	1.5	3	5	2	0.970	0.0382	1.08E−06	3.37E−02
c4	2	2	1.5	2	10	0.206	0.046	2.60E−06	2.32E−02
c5	2	2	2	5	3	0.873	0.0921	3.31E−06	2.54E−02
c6	2	2	3	1	10	0.514	0.1843	4.58E−06	6.13E−02
c7	2	3	1.5	5	4	0.667	0.153	7.82E−06	1.47E−02
c8	2	3	2	1	15	0.208	0.3058	9.20E−06	2.08E−02
c9	2	3	3	2	5	0.823	0.6117	1.12E−05	2.51E−02
c10	2	1.5	2	1	15	0.540	0.0191	7.36E−07	1.22E−01
c11	2	1.5	3	1	10	0.952	0.0382	1.08E−06	1.65E−01
c12	2	2	2	2	8	0.510	0.0921	3.31E−06	3.95E−02
c13	2	2	3	2	5	0.898	0.1843	4.58E−06	4.99E−02
c14	2	3	2	5	3	0.922	0.3058	9.20E−06	1.51E−02
c15	2	3	3	5	2	1.020	0.6117	1.12E−05	1.18E−02

$$D_h = \frac{2(1-X_T^{-1})}{X_T^{-1}} d \tag{15}$$

Substituting Eq. (15) into Eqs. (13) and (14) yields equations for the permeability and inertial coefficient of the square pin-fin heat sink, given $H \gg s$.

$$K_{PF} = \frac{8d^2}{(1+\chi)C} \frac{(1-X_T^{-1})^3}{X_T^{-2} X_L^{-1}} \tag{16}$$

$$F_{PF} = \frac{1}{\sqrt{(1+\chi)C/2}} \frac{(X_L^{-1})^{0.5}}{(1-X_T^{-1})^{0.5} X_T^{-1}} \times \frac{1+(n-1)\phi}{n} (Kc_{EF} + Ke_{EF}) \tag{17}$$

Moreover, when the square pin-fins are uniformly distributed (such that $X_T = X_L$), Eqs. (16) and (17) can be reduced as follows:

$$K_{PF} = \frac{8d^2}{(1+\chi)C} \left[\frac{1-\sqrt{1-\varepsilon}}{\sqrt{1-\varepsilon}}\right]^3 \tag{18}$$

$$F_{PF} = \frac{1}{\sqrt{(1+\chi)C/2}} \frac{1}{\left[\sqrt{1-\varepsilon}(1-\sqrt{1-\varepsilon})\right]^{0.5}} \times \frac{1+(n-1)\phi}{n} (Kc_{EF} + Ke_{EF}) \tag{19}$$

3. Experiments

This work involved a series of pressure drop tests, using the test equipment shown as Fig. 2, to evaluate the factor ϕ semi-empirically, and thus correct the pressure losses at the entrance and exit of internal fin rows to derive the permeability and inertial coefficient of the pin-fin heat sink. The blower supplies the airflow and the inverter controls the revolution of the motor to obtain different flow rates. After the air has entered the wind tunnel, it initially passes through an expansion section, before it enters the straightener. The straightened air flows into the test section, wherein the channel height is adjustable, before it leaves the wind tunnel. An anemometer is installed in the front section to measure the airflow speed, and a pressure transmitter is employed to measure the pressure drop as the air flows through the test section. The test section is 240 mm long and 120 mm wide, and contains an in-line pin-fin array. The pin-fin is made from 8 mm thick acrylic. The variable parameters

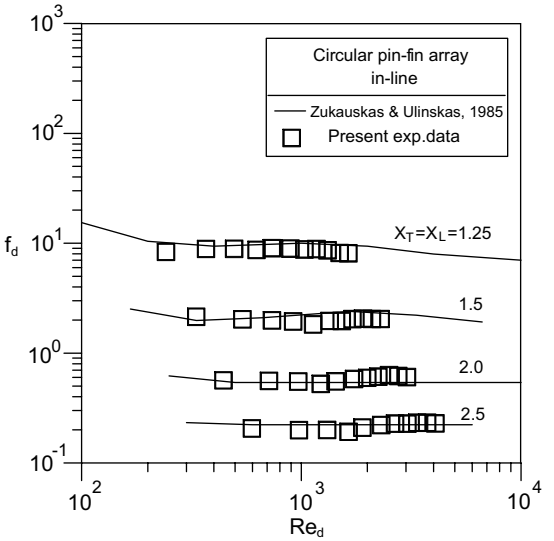

Fig. 3. Comparison with the other data for circular pin-fin arrays.

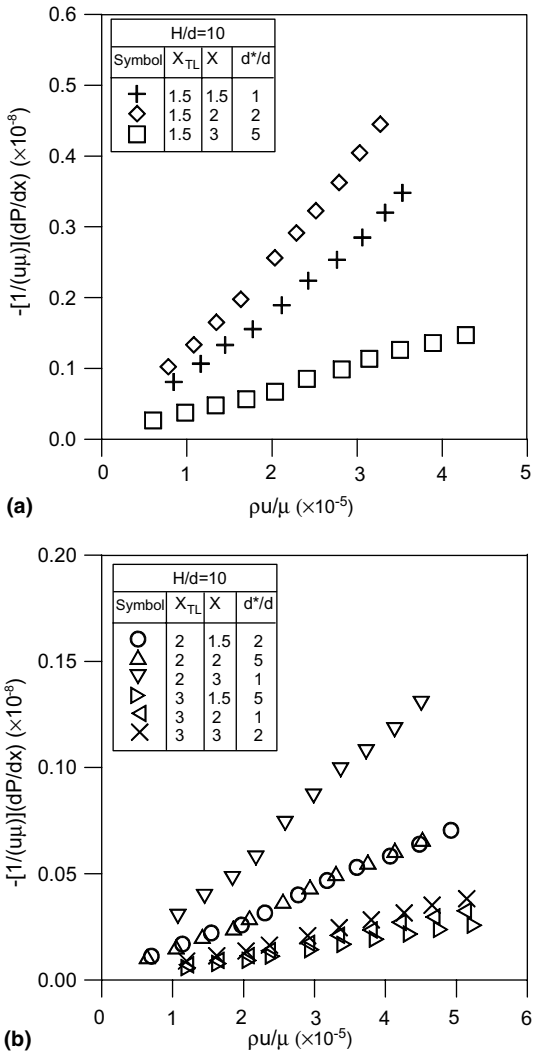

Fig. 4. Determination of permeability and inertial coefficient in $H/d = 10$. (a) $X_T = 1.5$ and (b) $X_T = 2.3$.

are the relative longitudinal pitch (X_L), the relative transverse pitch (X_T), the relative fin height (H/d) and the relative fin length (d^*/d). The values of the parameters are $X_L = 1.5, 2, 3$; $X_T = 1.5, 2, 3$; $H/d = 2, 5, 10$, and $d^*/d = 1, 2, 5$, respectively.

The pressure drops across the test sections at various airflow speeds are summarized into non-dimensional parameters as follows:

$$Re_d = \frac{\rho u d}{\mu}, \quad Da = \frac{K}{d^2}, \quad f_d = \frac{\Delta P}{0.5\rho u^2}\frac{d}{L} \tag{20}$$

where L is the length of the heat sink; d is the thickness of the fin or the diameter of the circular pin-fin, and u is the average Darcy velocity. Moreover, introducing the above dimensionless parameters into the Darcy friction factor (f_d). It can be expressed as follows:

$$f_d = 2\left(\frac{1}{Re_d Da} + \frac{F}{\sqrt{Da}}\right) \tag{21}$$

Furthermore, the standard single-sample uncertainty analysis recommended by Kline and McClintock [19] and Moffat [20] is used. Experimental results herein reveal that the average uncertainties in the Darcy friction factor and the Reynolds number are 2.92% and 2.59%, respectively.

4. Results and discussion

This work measures the pressure drops across pin-fin arrays with various X_T, X_L, H/d and d^*/d. A total of 45 pin-fin arrays are used. Table 1 lists the input parameters and semi-empirical results. The range of Reynolds numbers is $Re_d = 676$–$11{,}252$.

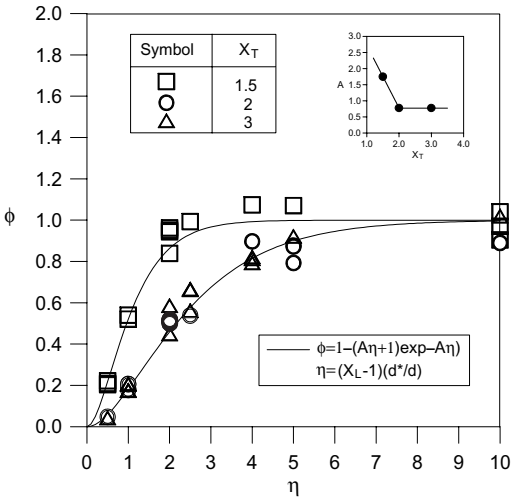

Fig. 5. Correlation of the drag factor ϕ in terms of X_T, X_L and d^*/d.

4.1. Validity of experiment

A test similar to that performed by Zukauskas and Ulinskas [14] is conducted to verify the accuracy of the experiment. The test section is an in-line pin-fin array; each pin-fin has a diameter of 8 mm and a height of 80 mm, whereas $X_T = X_L = 1.25$, 1.5, 2.0 and 2.5. Fig. 3 compares the present results and the other data for circular pin-fin arrays. The corresponding f_d for Re_d is consistent with the test results presented by Zukauskas and Ulinskas [14], indicating the accuracy of this test.

4.2. Determination of K and F

This work uses theory and testing to design a semi-empirical method to determine the permeability and

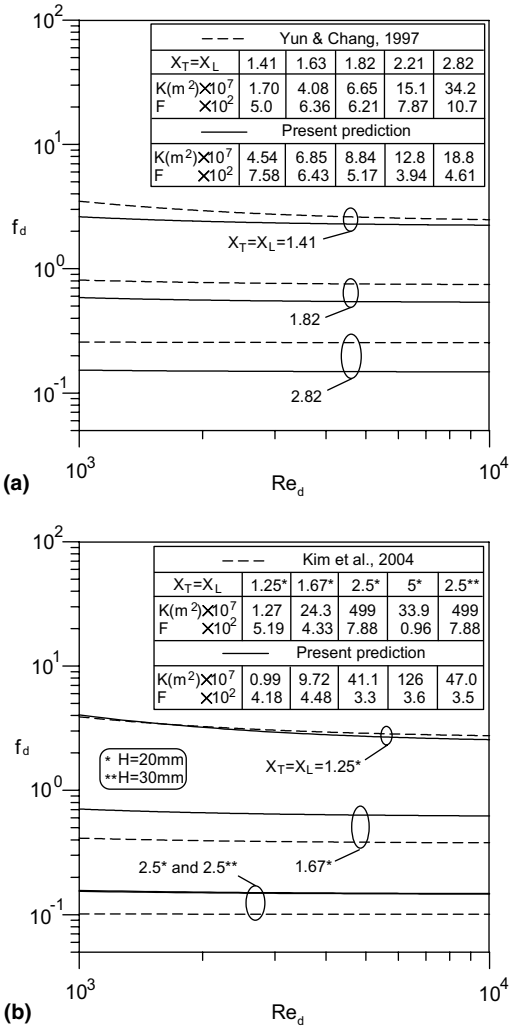

Fig. 6. Comparison with the data of other tests for square pin-fin arrays: (a) comparison with the data of You and Chang [15], (b) comparison with the data of Kim et al. [7].

inertial coefficient of the pin-fin heat sink. The method is similar to that presented by Hunt and Tien [16], who rearranged the modified Darcy equation to yield,

$$-\frac{1}{\mu u}\frac{\mathrm{d}p}{\mathrm{d}x}=\frac{1}{K}+\frac{\rho_f u}{\mu}\frac{F}{\sqrt{K}} \tag{22}$$

The permeability is obtained from the intercept and the inertial coefficient is determined from the gradient of a plot of the quantity $(-1/\mu u)(\mathrm{d}p/\mathrm{d}x)$ against $\rho_f u/\mu$ over a range of flow rates. Fig. 4 plots some experimental data to determine the permeability and inertial coefficient. Fig. 4 reveals that the test results indicate a strongly linear relationship between $(-1/\mu u)(\mathrm{d}p/\mathrm{d}x)$ and $\rho_f u/\mu$, but as X_T and X_L are increased, differentiating identifying the intercept becomes increasingly difficult. Accordingly, this work applies Eq. (13) to evaluate the permeability; then, the inertial coefficient can be obtained from the gradient, which can also be considered to determine the factor ϕ (Eq. (12)) to correct the pressure losses at the entrance and exit of internal fin rows. Table 1 presents the relevant semi-empirical results in present work. One of the important parameters is ϕ, as indicated in Section 2.2, in which the factor ϕ is assumed to be a function of X_T and $s^*(=(X_L-1)d^*)$, because the flow pattern into a row of the fin array is affected by the flow that exits from the previous row of the fin array and the longitudinal pitch between the fins. The factor ϕ normally equals one when each row of the fin array is assumed to be independent of the extruded-fin heat sink. The value of ϕ declines when the longitudinal distance between the adjacent fins is too short for the exit flow to expand uniformly. Fig. 5 presents the relationship between ϕ and X_T, X_L and d^*/d. It is expressed as follows:

$$\phi = 1-(1.747\eta+1)\mathrm{e}^{-1.747\eta} \quad \text{for} \quad X_T = 1.5 \tag{23}$$

$$\phi = 1-(0.775\eta+1)\mathrm{e}^{-0.775\eta} \quad \text{for} \quad X_T = 2,3 \tag{24}$$

$$\eta = (X_L-1)d^*/d \tag{25}$$

Fig. 5 reveals that the average deviation between the predictions of Eqs. (23)–(25) and the experimental data herein is 7.79%. The modified equation and the theory elucidated in Section 2 can be easily be applied to determine the permeability and inertial coefficient of the in-line pin-fin heat sinks with various values of X_T, X_L, H/d, and d^*/d. Fig. 6 compares the test results of You and Chang [15] and Kim et al. [7] with the estimates herein work. Table 2 presents the properties of some test cores employed by You and Chang [15] and Kim et al. [7]. It needs to note that the pressure changes at the inlet and exit of the pin-fin heat sink have been removed from the predictions by using the present method to compare with the data of Kim et al. [7]. Besides, the results are selected and plotted in separate multiple figures (such as Fig. 6(a) and (b)) with the same scale range for clearly comparing. The comparison reveals that, although the estimates of K and F differ from those provided by You and Chang [15] and Kim et al. [7], the change in f_d with Re_d remains reasonable by comparing with their data, indicating that the theory and semi-empirical method proposed herein can reasonably predict the permeability and inertial coefficient of the in-line pin-fin heat sink.

4.3. Effects of H/d, d*/d, X_T and X_L on pressure drop

This section considers the effects of relevant parameters on the pressure drop. Fig. 7 plots the non-dimensional pressure drop ($f_d Re_d^2$) as a function of Reynolds number. Within the range Re_d = 676–11,252, at a given Re_d, H/d negligibly affects the non-dimensional pressure drop. The pressure drop falls as d^*/d rises, especially

Table 2
Properties of test cores by You and Chang [15] and Kim et al. [7] for square pin-fin arrays

Test cores	Sample-1	Sample-2	Sample-3	Sample-4	Sample-5
You and Chang [15], $L = W = 0.12$ m, $H = 0.015$ m					
$d(=d^*)$ [m]	9.78E−3	6.33E−3	4.86E−3	3.29E−3	2.20E−3
$s(=s^*)$ [m]	4.0E−3	4.0E−3	4.0E−3	4.0E−3	4.0E−3
$X_T(=X_L)$	1.41	1.63	1.82	2.21	2.82
ε	0.462	0.599	0.679	0.782	0.865
n	9	12	14	17	20
Test cores	Sample-1	Sample-6	Sample-11	Sample-16	Sample-20*
Kim et al. [7], $L = W = 0.10$ m, $H = 0.020$ m					
$d(=d^*)$ [m]	9.02E−3	6.76E−3	4.51E−3	2.25E−3	4.51E−3
$s(=s^*)$ [m]	2.25E−3	4.51E−3	6.76E−3	9.02E−3	6.76E−3
$X_T(=X_L)$	1.25	1.67	2.5	5	2.5
ε	0.36	0.64	0.84	0.96	0.84
n	9	9	9	9	9

Note: *Presents H = 0.030 m.

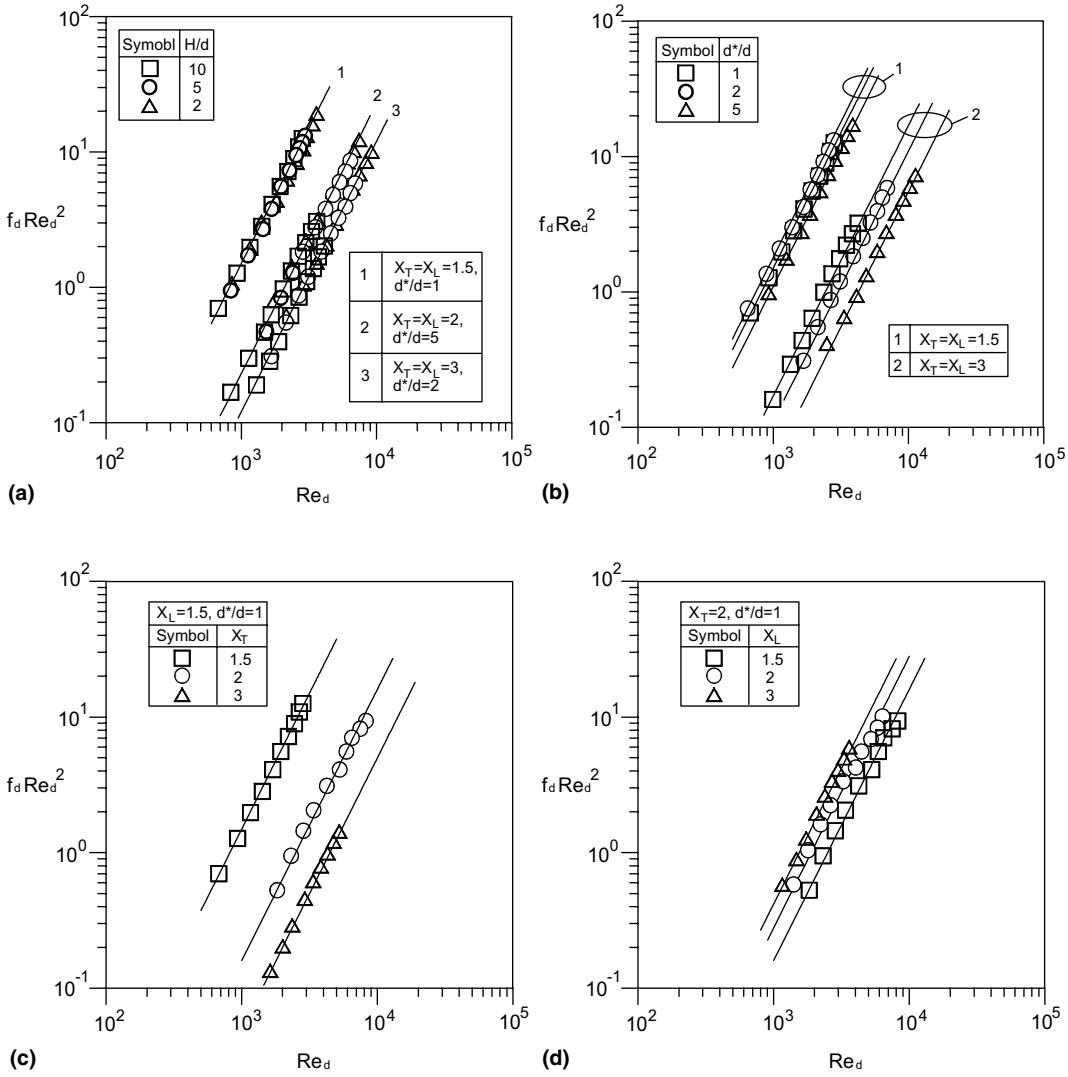

Fig. 7. Non-dimensional pressure drop as a function of Reynolds number in the effect of H/d, d^*/d, X_T and X_L: (a) effect of H/d, (b) effect of d^*/d, (c) effect of X_T, (d) effect of X_L.

when X_T and X_L are large. Additionally, the pressure drop increases as X_T decreases or X_L increases. This finding is consistent with the trend specified by Eq. (12) and Eqs. (23)–(25). Also, within this range of Re_d (Re_d = 676–11,252), the test results reveal that the main cause of the pressure drop is the form drag, which is the pressure loss at the inlet and the outlet of each row of fins, so the non-dimensional pressure drop ($f_d Re_d^2$) is proportional to Re_d^2.

5. Conclusions

This work elucidated the similarity between flow in a pin-fin heat sink and that in a porous media. A novel semi-empirical model of the permeability and inertial coefficient of pin-fin heat sinks is presented. The pressure drop across the pin-fin heat sinks in the rectangular channels is systematically and experimentally investigated. The variable parameters are the relative longitudinal pitch (X_L = 1.5, 2, 3), the relative transverse pitch (X_T = 1.5, 2, 3), the relative fin height (H/d = 2, 5, 10) and the relative fin length (d^*/d = 1, 2, 5). The following conclusions are drawn.

(1) Expressions for the permeability and inertial coefficient of pin-fin heat sinks are obtained using the presented semi-empirical model. Then, the compact pin-fin heat sinks could be regarded as the porous media and analyzed using the porous approach.

(2) The value of ϕ, the factor that corrects the pressure losses (or the form drag) at the entrance and exit of internal fin rows in the pin-fin array, declines as the longitudinal distance between the adjacent fins (=$(X_L - 1)d^*$) decreases. It increases as X_T declines.
(3) Within the range of Re_d (Re_d = 676–11,252), at a given Re_d, the effect of H/d on the non-dimensional pressure drop is negligible. The pressure drop declines as d^*/d increases, especially as X_T and X_L increase. Additionally, the pressure drop increases as X_T declines or X_L increases. The results are consistent with the theory.

Acknowledgement

The authors would like to thank the National Science Council of the Republic of China for financially supporting this research under Contract No. NSC 92-2212-E-344-005.

Appendix A

A.1. Extruded-fin heat sinks

$$\begin{aligned}\frac{\Delta P_{EF}}{L} &= \frac{1}{L}\frac{\rho u^{*2}}{2}\left[(Kc_{EF}+Ke_{EF})+\frac{C}{Re_D}\frac{L}{D_h}\right]\\ &= \frac{C}{\rho u^* D_h/\mu}\frac{\rho u^{*2}}{2D_h}+\frac{\rho u^{*2}}{2L}(Kc_{EF}+Ke_{EF})\\ &= \frac{\mu}{2D_h^2(1-X_T^{-1})/C}u+\frac{\rho(Kc_{EF}+Ke_{EF})}{2L(1-X_T^{-1})^2}u^2\\ &= \frac{\mu}{K_{EF}}u+\frac{\rho F_{EF}}{\sqrt{K_{EF}}}u^2 \end{aligned} \tag{A.1}$$

A.2. Pin-fin heat sinks

$$\begin{aligned}\frac{\Delta P_{PF}}{L} &= \frac{1}{L}\sum_{i=1}^{n}\left(\Delta P_{EF}+\frac{1}{2}\rho u^2\frac{C'}{Re'_D}\frac{s^*}{D'_h}\right)\\ &= \frac{1}{n(d^*+s^*)}\left[\sum_{i=1}^{n}\left(\frac{1}{2}\rho u^{*2}\frac{C}{Re_D}\frac{d^*}{D_h}+\frac{1}{2}\rho u^2\frac{C'}{Re'_D}\frac{s^*}{D'_h}\right)\right.\\ &\quad+\sum_{i=2}^{n}\frac{1}{2}\rho u^{*2}\phi Kc_{EF}+\sum_{i=1}^{n-1}\frac{1}{2}\rho u^{*2}\phi Ke_{EF}\\ &\quad\left.+\frac{1}{2}\rho u^{*2}(Kc_{EF}+Ke_{EF})\right]\\ &= \frac{d^*}{d^*+s^*}\frac{1}{d^*}\left[\left(\frac{1}{2}\rho u^{*2}\frac{C}{Re_D}\frac{d^*}{D_h}+\frac{1}{2}\rho u^2\frac{C'}{Re'_D}\frac{s^*}{D'_h}\right)\right.\\ &\quad\left.+\frac{1}{2}\rho u^{*2}\frac{1+(n-1)\phi}{n}(Kc_{EF}+Ke_{EF})\right]\\ &= \left[\frac{C(X_L^{-1})}{2D_h^2(1-X_T^{-1})}+\frac{C'(1-X_L^{-1})}{2(D'_h)^2}\right]\mu u\\ &\quad+\frac{X_L^{-1}}{2d^*(1-X_T^{-1})^2}\frac{1+(n-1)\phi}{n}(Kc_{EF}+Ke_{EF})\rho u^2\\ &= \frac{(1+\chi)C(X_L^{-1})}{2D_h^2(1-X_T^{-1})}\mu u+\frac{X_L^{-1}}{2d^*(1-X_T^{-1})^2}\frac{1+(n-1)\phi}{n}\\ &\quad\times(Kc_{EF}+Ke_{EF})\rho u^2\\ &= \frac{\mu}{K_{PF}}u+\frac{\rho F_{PF}}{\sqrt{K_{PF}}}u^2 \end{aligned} \tag{A.2}$$

$$\chi = \left(\frac{D_h}{D'_h}\right)^2\left(\frac{C'}{C}\right)\frac{(1-X_L^{-1})(1-X_T^{-1})}{X_L^{-1}} \tag{A.3}$$

References

[1] J.C.Y. Koh, R. Colony, Analysis of cooling effectiveness for porous material in coolant passages, ASME J. Heat Transfer 96 (1974) 324–330.
[2] K. Vafai, C.L. Tien, Boundary and inertial effects on flow and heat transfer in porous media, Int. J. Heat Mass Transfer 24 (1981) 195–203.
[3] J.C.Y. Koh, R. Colony, Heat transfer of microstructures for integrated circuits, Int. Commun. Heat Mass Transfer 13 (1986) 89–98.
[4] H.I. You, C.H. Chang, Numerical prediction of heat transfer coefficient for a pin-fin channel flow, ASME J. Heat Transfer 119 (1997) 840–843.
[5] S.J. Kim, D. Kim, Forced convection in microstructures for electronic equipment cooling, ASME J. Heat Transfer 121 (1999) 639–645.
[6] D. Kim, S.J. Kim, Compact modeling of fluid flow and heat transfer in straight fin heat sinks, ASME J. Electron. Packag. 126 (2004) 247–255.
[7] D. Kim, S.J. Kim, A. Ortega, Compact modeling of fluid flow and heat transfer in pin fin heat sinks, ASME J. Electron. Packag. 126 (2004) 342–350.
[8] J. Bear, Dynamics of Fluids in Porous Media, Dover, NY, 1972, pp. 119–186.
[9] J. Bear, A. Verruijt, Modeling Groundwater Flow and Pollution (Theory and Applications of transport in Porous Media), D. Reidel, Holland, 1987, pp. 27–43.
[10] S. Ergun, Fluid flow through packed columns, Chem. Eng. Progr. 48 (1952) 89–94.
[11] J.E. Drummond, M.I. Tahir, Laminar viscous flow through regular arrays of parallel solid cylinders, Int. J. Multiphase Flow 10 (1984) 515–540.
[12] A.J. Fowler, Fundamental topics in heat transfer through deformable two-phase media, PhD thesis, Duke University, Durham, NC, 1993.
[13] A.R. Martin, C. Saltiel, W. Shyy, Heat transfer enhancement with porous inserts in recirculating flows, ASME J. Heat Transfer 120 (1998) 458–467.
[14] A. Zukauskas, R. Ulinskas, Efficiency parameters for heat transfer in tube banks, Heat Transfer Eng. 6 (1985) 19–25.
[15] H.I. You, C.H. Chang, Determination of flow properties in non-Darcian flow, ASME J. Heat Transfer 119 (1997) 190–192.

[16] M.L. Hunt, C.L. Tien, Effects of thermal dispersion on forced convection in fibrous media, Int. J. Heat Mass Transfer 31 (1988) 301–309.
[17] A.F. Mills, Basic Heat and Mass Transfer, Richard D. IRWIN Inc., Chicago, 1995, pp. 630–631.
[18] A.J. Chapman, Fundamentals of Heat Transfer, Macmillion, NY, 1987, p 261.
[19] S.J. Kline, F.A. Mcclintock, Describing uncertainties in single-sample experiments, Mech. Eng. (1953) 3–8.
[20] R.J. Moffat, Contributions to the theory of single-sample uncertainty analysis, ASME J. Fluids Eng. 104 (1986) 250–260.